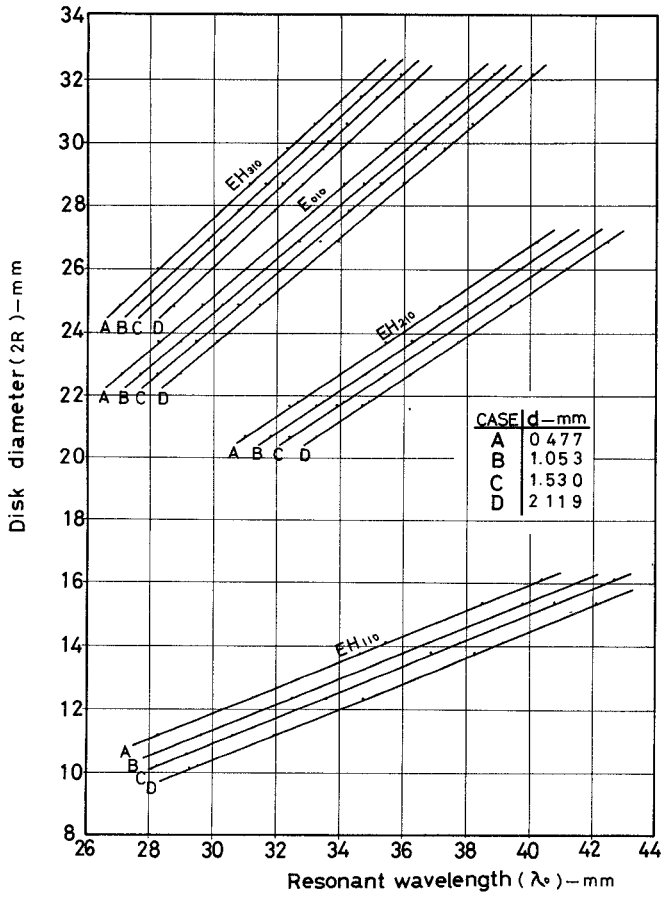

Fig. 2. The measured resonant wavelength for some lowest modes versus disk diameter in the four cases of teflon thickness (d).

probable error 0.2 percent. We could not find any appreciable discrepancies among experimental values measured at various ratios between 5 and 30 for the different modes.

V. CONCLUSION

We have carried out the numerical analysis only for a few lowest *E*- and *EH*-modes, which can be easily excited by simple means [1], [2], [8] and may be useful for the practical usages. However, we remark that the *HE*-mode also obeys (16), and its eigenvalue is obtainable in a similar way. Thus our method of series expansion can be utilized for any resonance mode of our disk resonator.

The applicabilities of the Marcuvitz method and the approximated Marcuvitz method are limited to the region of large ratios. In particular, the latter contains considerable error at small ratios. The difficulty of finding some approximation method at small ratios is implied by slow convergence to the exact value of eigenvalue according as increasing dimensionality of approximate determinant, namely by the significant admixture of the higher harmonics.

ACKNOWLEDGMENT

The authors wish to thank Y. Suzuki a student of Saitama University for his assistance in this experiment.

REFERENCES

[1] Y. Kobayashi, "The resonators applied on strip lines," *Rec. Professional Groups, Inst. Electron. Commun. Eng. Japan*, Paper MW 70-64, pp. 1–10, Jan. 1971.
[2] Y. Kobayashi, T. Oikawa, and S. Tanaka, "Disk resonator applied to balanced strip line," *Rec. Inst. Electron. Commun. Eng. Japan*, Paper 521, Apr. 1971.
[3] T. Okoshi and T. Miyoshi, "The planar circuit—An approach to microwave integrated circuitry," *IEEE Trans. Microwave Theory Tech.*, vol. MTT-20, pp. 245–252, Apr. 1972.
[4] N. Marcuvitz, *Waveguide Handbook*. Cambridge, Mass.: Boston Tech., 1964.
[5] T. Makimoto, M. Yamamoto, and Y. Sugita, "Resonant frequency and *Q*-factor of triple plate disk resonator," *Rec. Inst. Electron. Commun. Eng. Japan*, Paper 519, Apr. 1971.
[6] T. Miyoshi and T. Okoshi, "Analysis of microwave planar circuit," *Trans. Inst. Electron. Commun. Eng. Japan*, vol. 55-B, no. 8, pp. 441–448, Aug. 1972.
[7] J. O. Stratton, *Electromagnetic Theory*. New York: McGraw-Hill, 1941.
[8] Y. Kobayashi, K. Tanabe, and S. Tanaka, "Discussions on the measurement of dielectric constant using disk resonator," *Rec. Inst. Electron. Commun. Eng. Japan*, Paper 617, Apr. 1973.

A New Class of Nonreciprocal Components Using Slot Line

L. COURTOIS AND M. DE VECCHIS

***Abstract*—The authors present an experimental and theoretical study of edge modes in a ferrite-loaded slot line. Nonreciprocal properties are obtained over a broad frequency band. Added microstrip lines provide suitable transitions.**

A theory based on magnetic boundary conditions shows good agreement with the experimental results and allows a comparison with stripline devices described by Hines. In particular, the characteristics of the slot-line isolators are satisfactorily explained by this theory.

I. INTRODUCTION

It is well known [1], [2] that the dominant mode in a slot line exhibits regions where the magnetic field is elliptically polarized both in the substrate and in the air outside the substrate. It is possible to utilize this property to the design of nonreciprocal microwave components such as isolators using a resonance effect. However, such a device does not offer a broad frequency band of operation.

In this short paper we will demonstrate that it is possible to obtain nonreciprocal behavior due to an integral field-displacement effect over a broad frequency band with a device using a slot line on a ferromagnetic substrate [3].

II. EXPERIMENTAL STUDY OF THE DEVICE

Our initial experiments with various slot-line geometries led to the selection of the suitable structure shown in Fig. 1. Using such a device, we have performed experiments using liquid crystals in order to demonstrate the field-displacement effect. Liquid crystals are deposited on the two sides of the device, with the absorbent removed, and they act as a transducer permitting visualization of the electromagnetic energy [4]. If we designate an input and an output, it appears that for a given applied dc field, the direct energy is traveling along one side while the reverse energy is traveling along the other side. Consequently, we can hypothesize an energy distribution inside the ferrite, as shown in Fig. 1(b). The alumina substrate in Fig. 1(a) is especially helpful in reducing the insertion losses of the device.

Manuscript received June 18, 1974; revised December 2, 1974. This work was supported by the French Air Force Telecommunication Technical Service (STTA).

L. Courtois is with the Laboratoire de Magnetisme et d'Optique des Solides, Centre National de la Recherche Scientifique, Meudon Bellevue, France.

M. de Vecchis is with the Departement Hyperfrequences, LTT, Conflans Sainte Honorine, France.

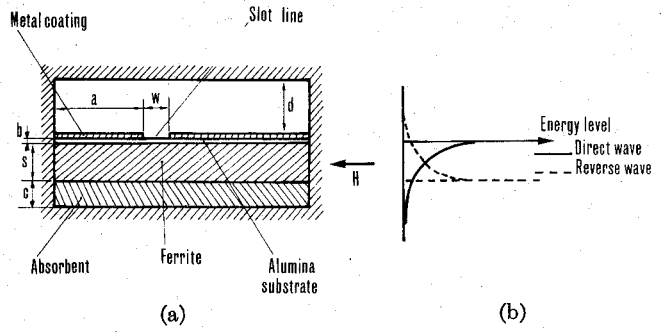

Fig. 1. (a) Structure of the device. (b) Distribution of energy in the ferrite slab.

The slot line has been extensively described [1], [2], [5], [6] and it is known that a number of constraints exist concerning its parameters. For example, near the edges of the slot there is a finite surface-current density. Consequently, the value of the distance (a) between the side wall and the edge of the slot cannot be reduced to zero. Likewise, the value of the parameter (d) must be chosen to take into account the slot-line field components in the air [1], [7].

The ratio S/W is an important parameter. Direct losses and isolation are poor if this ratio is too small, as shown in Fig. 2. A minimum value of $S/W = 5$ is necessary to obtain characteristics worthy of acceptance with a YIG substrate, and a value of $S/W = 8$ is in many cases a good choice.

The absorbent is obviously an important parameter affecting isolation, and Fig. 3 shows its influence. The material used for these experiments was made of iron powder.

The sensitivity of the device to variations of applied dc field is represented in Fig. 4, where direct losses and isolation at 4 GHz are plotted versus the ratio between applied dc field and resonance field at 4 GHz.

Another important problem is the design of the transition between the slot line and coaxial lines. Cohn has described two such transitions [1]. The first is between slot line and a miniature semirigid coaxial line, but the losses of this transition using a YIG substrate are rather large [2]. The second one is between a slot line and a microstrip, but it is not feasible with the structure described in Fig. 1 because of the relatively large value of the height of the ferrite substrate S. We have developed a new type of transition shown in Fig. 5. The ground plane of a 50-Ω microstrip line is bonded near one edge of the slot. The other edge is connected to the microstrip line by means of a gold strip. The characteristics of such a transition are very satisfactory for frequencies up to more than 11 GHz. An isolator using two transitions of this type is shown in Fig. 6.

III. THEORETICAL STUDY

In order to explain the characteristics of this device, we present a description of the modes occurring in the structure. When symmetry consideration and the effects of losses are taken into account, the mode spectrum predicted is in good agreement with our experiments.

The theory is based on a fundamental hypothesis, similar to Hines's assumption concerning stripline devices [8]. We assume that the boundary plane between the ferrite substrate and the slot line is equivalent to a magnetic wall.

The RF magnetic field is orthogonal to the electric field, which is in the plane of the slot. Consequently, the slot can be considered as a magnetic wall. This is obviously not true in all the slot plane; nevertheless, the hypothesis agrees with experimental results in the slot line as well as in the stripline configuration.

We have studied the modes propagating along a ferrite slab with magnetization parallel to an axis of the slab (Fig. 7). The slab thickness t is limited by two metallic walls and height S by a magnetic

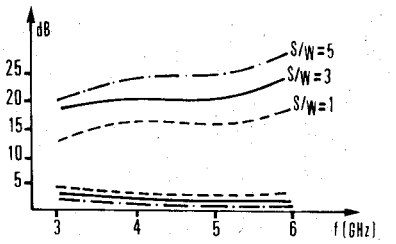

Fig. 2. Influence of ratio S/W, $W = 0.9$ mm, $a = 9$ mm, $b = 0.635$ mm, $e \geq 6$ mm, length of the slot line $l = 40$ mm.

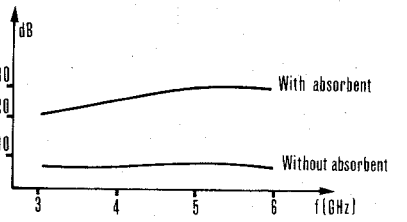

Fig. 3. Influence of absorbent on isolation. The dimensions have the same values as in Fig. 2. $S/W = 8$.

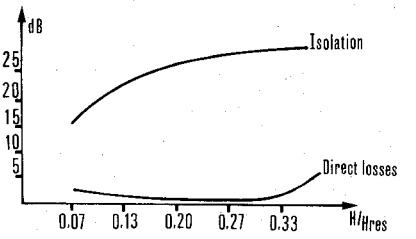

Fig. 4. Performance versus applied dc field ($f = 4$ GHz). The dimensions have the same values as in Fig. 3.

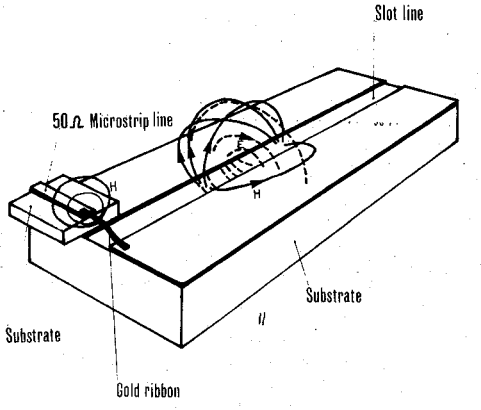

Fig. 5. Transition with added microstrip line.

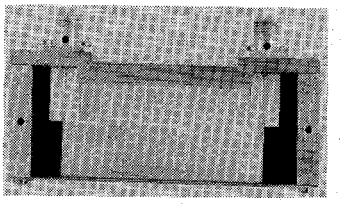

Fig. 6. Photograph of the isolator showing the transitions (magnets removed). The dimensions have the same values as in Fig. 3.

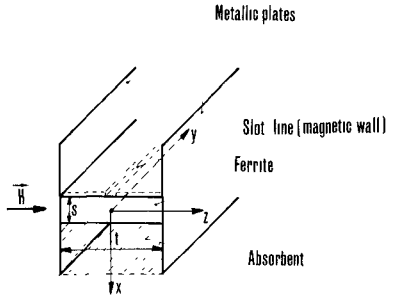

Fig. 7. Ferrite-slab geometry.

wall and dissipative medium of impedance Z and refractive index N_d

$$Z = \left(\frac{\mu_d}{\mu_0}\frac{\epsilon_0}{\epsilon_d}\right)^{1/2}$$

and

$$N_d = \left(\frac{\epsilon_d}{\epsilon_0}\frac{\mu_d}{\mu_0}\right)^{1/2}. \tag{1}$$

In this structure the mode configuration can be written using only trigonometric and hyperbolic functions. The modes of the slab are slow modes and, taking into account the symmetry plane xoy, the field components are space functions

$$\left.\begin{array}{l}\text{ferrite} \sum_{1,2} A_{1,2} \cos\left(k_{xf_{1,2}} x + \psi_{1,2}\right) \\ \text{dissipative medium } \exp\left(-k_{xd} \cdot x\right)\end{array}\right\} \cdot \begin{Bmatrix}\cos \\ \sin\end{Bmatrix} (k_z \cdot z) \exp\left[j(\omega t - k_y \cdot y)\right] \tag{2}$$

where integers 1 and 2 correspond to ordinary and extraordinary waves. Boundary conditions on the two conductors lead to

$$k_z t = n\pi \tag{3}$$

where n is an integer ≥ 0.

Case $k_z = 0$

The case $n = 0$ is now well known [8]–[10]. The modes split into TE and TM modes (TM modes occur only if t approaches infinity). The xoz plane has no symmetry property; nevertheless, the modes can still be characterized by an index m so that

$$k_{xf} \simeq m\pi. \tag{4}$$

The anisotropic properties of the ferrite allow solutions exhibiting an imaginary transverse component k_{xf} of the wave vector. These modes are TE, and the electromagnetic fields decrease exponentially from the side of the slab. These modes are called edge modes or surface modes, and have been previously described [8], [9].

Case $k_z \neq 0$

The theoretical study of the case $k_z \neq 0$ is slightly more sophisticated. It has been accomplished [11], but will be republished shortly in a more complete manner. The modes are neither TE nor TM but hybrid. In the dissipative medium every mode can be considered as a linear combination of TE and TM waves; in the same way, every mode in the ferrite can be considered as a linear combination of ordinary and extraordinary waves.

Boundary conditions of continuity lead to a linear and homogeneous 8×8 system.

Setting the determinant of the coefficients equal to zero gives the characteristic equation. To each zero corresponds an eigenmode characterized by a propagation vector k_y.

The modes are labeled as HE_{nm} and HM_{nm} so that, if thickness $t \to \infty$, these modes are, respectively the same as TE_m and TM_m modes.

Discussion of Dispersion Curves

We performed a numerical study from the physical data of the structure as listed in the following table:

Polycrystalline YIG Slab
Height: $S = 0.8$ cm
Thickness: $t = 2.4$ cm
Magnetization: $4\pi Ms = 1780$ G
Internal dc field: $H = 400$ Oe
Gyromagnetic ratio: $\gamma = -2.8$ MHz/Oe
Permittivity: $\epsilon_f = 14.5\ \epsilon_0$
Electrical loss tangent: $\tan\delta = 2 \cdot 10^{-4}$
Effective linewidth: $\Delta H_{eff} = 5$ Oe
Dissipative Medium
Complex permittivity: $\epsilon_d = 14\ (1 - j)\epsilon_0$
Complex permeability: $\mu_d = (1 - j)\mu_0$

Dispersion curves for low-index (n,m) modes are presented in Fig. 8. The symmetry of the device, which is achieved by a high degree of precision in its manufacturing, especially in the adjustment of the coupling loops, prevents the excitation of odd (n) modes as well as any HM modes.

In the frequency range from 3 to 6 GHz, where we have tested the structure, the device is multimode. The TE_{01} mode, which is actually a surface mode, is unidirectional and permits good operation of the slot-line isolator. On the other hand, the HE_{21} mode is partially a surface mode because k_{xf} extraordinary is imaginary, but k_{xf} ordinary is real. Consequently, it is impossible to place a dissipative load on a side of the ferrite slab without attenuating this mode. Therefore, to understand more clearly how this device operates, it is necessary to introduce some loss into the theoretical treatment. In the use of complex calculus, the theory and the formulas are the same as in the case where losses are neglected. The losses which are introduced have three origins.

1) Dielectric losses in the ferrite, characterized by a complex permittivity $\epsilon'(1 - j\tan\delta)$.

2) Magnetic losses, characterized by a complex magnetic dc field $H + (j/2)\,\Delta H_{eff}$, where ΔH_{eff} is the effective linewidth.

3) Losses due to the dissipative medium.

The surface mode TE_{01} is weakly affected by the three types of losses just described, but the other modes are considerably damped by the dissipative medium.

Fig. 9 shows attenuation for the low-index (n,m) modes.

IV. COMPARISON BETWEEN THEORY AND EXPERIMENTAL RESULTS

The isolator shown in Fig. 6 has been tested on a Hewlett- Packard automatic network analyzer. Results concerning direct losses, isolation, and VSWR are shown in Fig. 10.

We also show in Fig. 8 the measured values of phase introduced by the device. The curve obtained is parallel to the theoretical curve of the TE_{01} mode. This good agreement between experimental results and theory demonstrates that energy is located essentially in the ferrite in accordance with our assumptions.

This device and the corresponding theory can be compared to stripline devices [8], [9], and at first sight it seems to be possible to reduce the thickness t and thus obtain a similar device, except for the excitation. However, as we have seen (Section II) it is necessary to avoid a large change in the slot-line field components, thus making it mandatory to maintain a minimum distance between slot line and side walls.

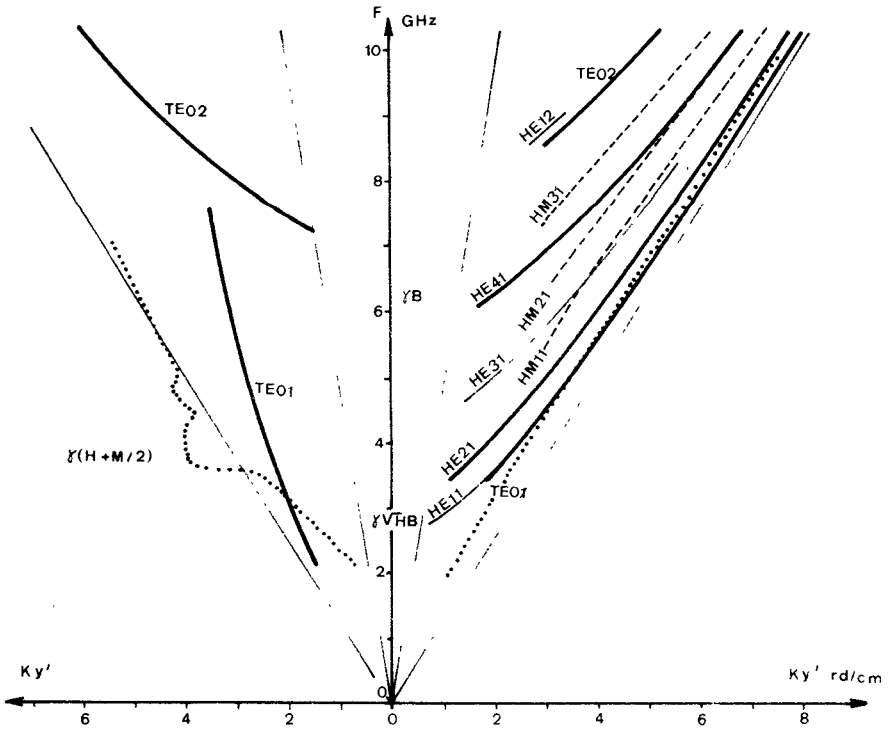

Fig. 8. Theoretical dispersion curves (direct and reverse). The dotted lines show experimental results. Thick continuous lines are related to even HE modes. Thin continuous lines are related to odd HE modes. Dash lines are related to HM modes.

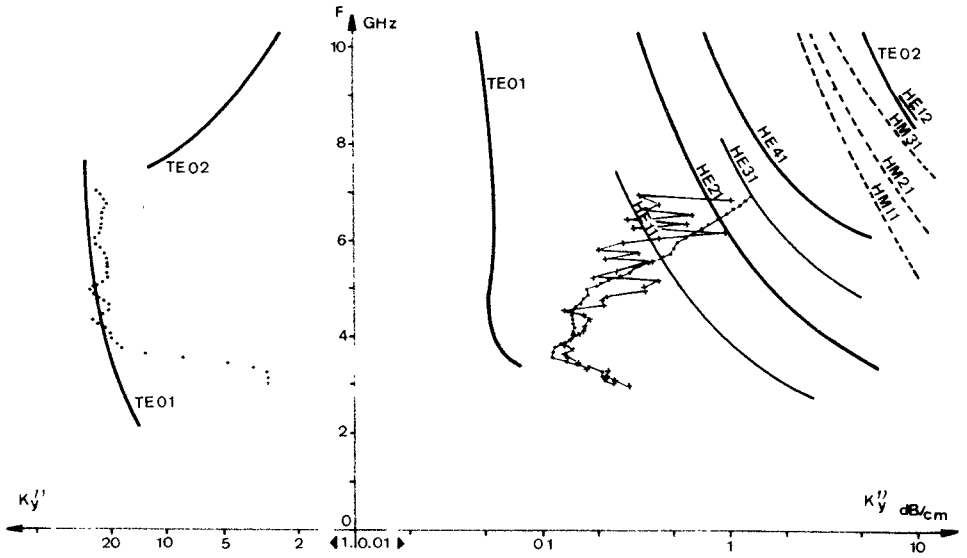

Fig. 9. Attenuation for the low-index modes (theoretical and experimental). See Section IV of text.

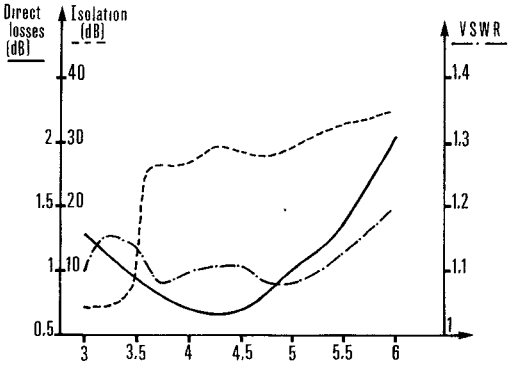

Fig. 10. Performance of the isolator shown in Fig. 6.

The value of the thickness t is an important difference between strip- and slot-line devices and creates an obvious limitation to higher frequency operation; i.e., n-order modes can be propagated that do not exhibit properties of surface-energy concentration like that of the TE_{01} mode.

Direct Losses

Fig. 9 is related to the losses of the device. Theoretical losses and measured losses of the complete device and the device without absorbent are plotted. Theoretical losses are calculated for the fundamental mode TE_{01} and the first parasitic modes. If we suppose that each mode is excited proportionally to $Q^{1/2}$ where

$$Q = \frac{k_y'}{2k_y''}$$

is the quality factor of this mode, the HE_{21} mode will be excited more easily as the frequency increases and thus an energy transfer towards the load appears which increases the insertion losses. If the dissipative load is removed, the modes sometimes add and sometimes subtract so that an oscillation appears in the insertion losses. When the mode HE_{41} can be propagated, losses increase again and the device ceases to operate.

At low frequencies, the device is equivalent to the stripline device and low field losses are the only transmission limitation.

Isolation

The isolation curve at low frequency of the slot-line device shows that transmission occurs in the reverse direction. This transmission is characterized by a long delay, the phase curve being quite horizontal on the dispersion diagram (see Fig. 8). This phenomenon appears at a very well-defined frequency and the decrease in isolation is very abrupt (see Fig. 10 for $f = 3.6$ GHz). It depends on the applied dc field and the saturation magnetization of the ferrite. Its origin is not to be found in a dimensional resonance of the device but rather in the presence of a parasitic mode. We have recognized a magnetostatic mode TE_{00}, described by Damon and Eshbach [12]. We know that this mode propagates in the reverse direction to that of the TE_{01} dynamic mode and is related to the gyromagnetic resonance phenomenon. The high permeability permits a very short wavelength. Consequently, the hypothesis that the slot is a magnetic wall is only true near the edges of the slot. Thus a magnetostatic mode can be propagated and such a mode exhibits a pole for a frequency

$$\frac{F_p}{\gamma} = H + \frac{M_0}{1 + \mu_d/\mu_0} = H + \frac{M_0}{2}. \tag{5}$$

This relation gives the internal dc field which we have found using our theoretical calculation to be 400 Oe. This is in good agreement with the experimentally determined value.

V. OTHER EXPERIMENTAL RESULTS

It was also found that the absorbent is replaceable by a ferrite used in a lossy region of polarization (Fig. 11). For instance, the field H' may be equal to zero. The ferrite used as an absorbent may be the same as the main ferrite but the field H' is then different from the field H.

Another method of separating the direct and reverse waves is the use of a slot line deposited on the second side of the device instead of the absorbent, and suitably loaded (Fig. 12). If the widths of the slot lines are equal, and if the second slot line is matched by using coaxial transitions or the transitions described in Section II, we obtain a four-port circulator. The first experimental results achieved with this device are as follows:

1) central frequency: 4 GHz;
2) bandwidth: 1 GHz;
3) direct losses: ≤ 3 dB;
4) isolation: ≥ 25 dB.

Experiments have shown that these results may be improved by optimizing the geometrical parameters of the device and we are currently working on defining an optimum set of parameters. Such a circulator seems to offer an easier way to obtain broad-band circulators than devices using stripline geometry.

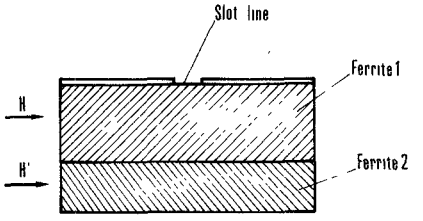

Fig. 11. Use of a second ferrite as an absorbent.

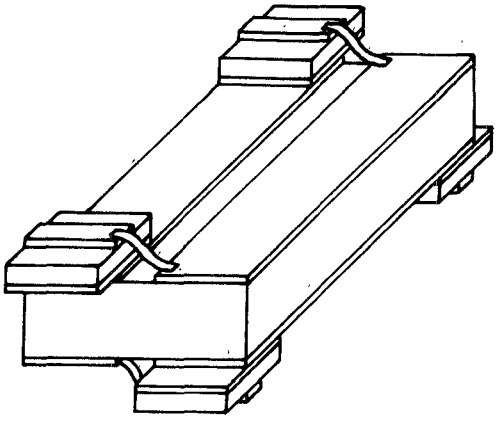

Fig. 12. Four-port slot-line circulator.

VI. CONCLUSION

A study has been made of a new type of nonreciprocal component. The nonreciprocal behavior has been demonstrated and theoretical predictions have been found to be in good agreement with experimental results. Future developments of these devices are being considered and it seems that they offer a more attractive solution to the problem of mode transformation than is possible using stripline structures.

ACKNOWLDEGMENT

The authors wish to thank B. Chiron, Director of the Microwave Department at LTT, for valuable discussions and guidance.

REFERENCES

[1] S. B. Cohn, "Slot line on a dielectric substrate," *IEEE Trans. Microwave Theory Tech.*, vol. MTT-17, pp. 768–778, Oct. 1969.
[2] G. H. Robinson and J. L. Allen, "Slot line applications to miniature ferrite devices," *IEEE Trans. Microwave Theory Tech. (1969 Symposium Issue)*, vol. MTT-17, pp. 1097–1101, Dec. 1969.
[3] M. de Vecchis, L. Raczy, and P. Gelin, "A new slot line broadband isolator," in *Proc. European Microwave Conf.* (Brussels, Belgium, 1973).
[4] J. Puyhaubert, "Visualisation des ondes électromagnétiques hyperfréquences à l'aide de cristaux liquides," *Onde Elec.*, vol. 52, p. 213, May 1972.
[5] E. A. Mariani, C. P. Heinzman, J. P. Agrios, and S. B. Cohn, "Slot line characteristics," *IEEE Trans. Microwave Theory Tech. (1969 Symposium Issue)*, vol. MTT-17, pp. 1091–1096, Dec. 1969.
[6] J. C. Minor, "Modes in the shielded microstrip and microslot on a ferrite substrate magnetized transverse to the direction of propagation and in the plane of the substrate," M.S. thesis, Brown Univ., Providence, R. I., June 1971.
[7] S. B. Cohn, "Slot-line field components;" *IEEE Trans. Microwave Theory Tech.* (Corresp.), vol. MTT-20, pp. 172–174, Feb. 1972.
[8] M. E. Hines, "Reciprocal and nonreciprocal modes of propagation in ferrite stripline and microstrip devices," *IEEE Trans. Microwave Theory Tech.*, vol. MTT-19, pp. 442–451, May 1971.

[9] L. Courtois, B. Chiron, and G. Forterre, "Propagation dans une lame de ferrite aimantée. Application à de nouveaux dispositifs non réciproques à large bande," *Cables Transmission*, pp. 416–435, Oct. 1973.
[10] T. J. Gerson and J. S. Nadan, "Surface electromagnetic modes of a ferrite slab," *IEEE Trans. Microwave Theory Tech.*, vol. MTT-22, pp. 757–763, Aug. 1974.
[11] L. Courtois, "Propagation oblique des ondes électromagnétiques dans une lame de ferrite aimantée parallèlement à ses faces," *Electron. Fis. Apl.*, vol. 16, pp. 286–294, Apr./June.
[12] R. W. Damon and J. R. Eshbach, "Magnetostatic modes of a erromagnetic slab," *J. Phys. Chem. Solids*, vol. 19, p. 308, 1961.

The Edge-Guided-Wave Circulator

P. DE SANTIS AND F. PUCCI

***Abstract*—A complete study is presented on "edge-guided-wave" circulators (EGC). The fundamental physical principles which underlie EGC's operation are established and exploited to construct a broad-band circulator in the 8–12-GHz band. The performance data are compared to those of a "continuous tracking" circulator (CTC) and a traditional *Y*-junction circulator.**

I. INTRODUCTION

Since 1971 a number of people have become interested in fabricating a three-port symmetrical microwave integrated circuit (MIC) circulator based on edge-guided-wave (EGW) propagation [1]–[6]. This type of propagation in MIC circuits deposited on a substrate of magnetized ferrite was originally studied by Hines [1]. It is based on a transversal field displacement effect which concentrates the electromagnetic (EM) field at one of the edges of the strip conductor for one sense of propagation and at the other edge for the opposite sense of propagation. One of the most attractive characteristics of EGW is that it is extremely broad band [2]. Although in principle one may think of exploiting EGW in a number of nonreciprocal passive devices, from the very beginning it turned out that some difficulties existed in having these waves circulate along curved edges, and that magnetic losses drastically limited the bandwidths predicted by theory [4], [5]. More specifically, laboratory experiments evidenced that EGW propagation along curved paths was plagued by the existence of spurious-volume mode resonances. That was the main reason why efficient EGW broad-band isolators were readily constructed, whereas no broad-band EGW circulator has as yet appeared which could outperform the traditional *Y*-junction MIC circulators.

On the other hand, a significant step forward in the construction of broad-band MIC circulators was recently made with the discovery of the continuous tracking principle [7].

It is the purpose of this work to present a complete study on the EGW circulator (EGC) beginning by clearly stating what it is and how it compares to other broad-band MIC circulators. A theoretical analysis on EGW along curved edges will be subsequently introduced, which is of relevance in understanding the performance of the EGC.

Finally, the performance data of a three-port EGC will be presented and compared with those of other types of MIC broad-band *Y*-junction circulators.

Manuscript received July 31, 1974; revised November 27, 1974.
The authors are with the Research Department, Selenia S.p.A., Rome, Italy.

II. DEFINITION OF EGW CIRCULATOR

MIC *Y*-junction circulators consist of a circular junction, which is the nonreciprocal part of the device, connected to the three ports of the device by means of suitable impedance transformers [Fig. 1(a)]. Under these circumstances only the circular junction or a slightly larger region is required to be magnetically active; i.e., realized with magnetized ferrite (shaded area). The impedance transformers are deposited on an isotropic substrate. An EGC is constituted by a suitably shaped MIC circuit [see Fig. 1(b)] deposited on a magnetically active substrate; i.e., both in the central part and in the impedance transformers nonreciprocal action takes place. Therefore a peculiar characteristic of the EGC is that, at variance with other types of circulators, a lateral field displacement effect occurs in the impedance transformers. Note that in an EGC the coupling angle 2ψ is always $2\pi/3$. Furthermore, from Fig. 1(b) it is apparent that in the EGC, the distinction between circular junction and impedance transformers is a fictitious one and that a modal expansion in terms of Bessel's functions is no longer valid.

Under these circumstances a modal analysis of the EGC seems to be rather involved, and approximate analytical techniques applied to simplified models seem to be in order.

III. EGW PROPAGATION ALONG CURVED EDGES

In the absence of an exact solution for the boundary value problem associated with an EGC, some useful information can be gathered from the analysis of simplified models. Obviously, the most elementary model that one can think of is the curved edge of a semi-infinite strip conductor deposited on a ferrite substrate (Fig. 2). Such a geometry has already been studied by one of the authors [8] and here only those results which are of relevance to the study at hand will be reported.

With reference to Fig. 2, if a Z-independent EM field is assumed, TM_Z modal solutions are possible and all field components can be derived from the Z component of the electric field which is given by

$$E_Z(r,\theta) = AH_n^{(2)}(K_f r) \exp(\pm jn\theta) \tag{1}$$

$$K_f = \frac{\omega}{C}(\mu_{\text{eff}}\epsilon_f)^{1/2}. \tag{2}$$

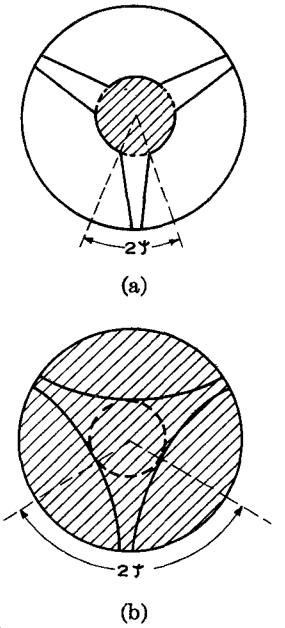

Fig. 1. Relevant to the definition of EGC. The shaded area represents the magnetically active region. $2\psi = 2\pi/3$ is the coupling angle.